MOLECULAR AND CELLULAR BIOLOGY, Apr. 2007, p. 2423–2430 Vol. 27, No. 7
0270-7306/07/$08.00+0 doi:10.1128/MCB.01111-06

Iron-Dependent Degradation of Apo-IRP1 by the Ubiquitin-Proteasome Pathway▽

Jian Wang,[1]¶† Carine Fillebeen,[1]† Guohua Chen,[1]# Annette Biederbick,[2] Roland Lill,[2] and Kostas Pantopoulos[1,3]*

Lady Davis Institute for Medical Research, Sir Mortimer B. Davis Jewish General Hospital, 3755 Cote-Ste-Catherine Road, Montreal, Quebec H3T 1E2, Canada[1]; Institut für Zytobiologie, Philipps Universität Marburg, Robert Koch Str. 6, 35037 Marburg, Germany[2]; and Department of Medicine, McGill University, Montreal, Quebec, Canada[3]

Received 20 June 2006/Returned for modification 1 August 2006/Accepted 12 January 2007

Iron regulatory protein 1 (IRP1) controls the translation or stability of several mRNAs by binding to "iron-responsive elements" within their untranslated regions. In iron-replete cells, IRP1 assembles a cubane iron-sulfur cluster (ISC) that inhibits RNA-binding activity and converts the protein to cytosolic aconitase. We show that the constitutive $IRP1_{C437S}$ mutant, which fails to form an ISC, is destabilized by iron. Thus, exposure of H1299 cells to ferric ammonium citrate reduced the half-life of transfected $IRP1_{C437S}$ from ~24 h to ~10 h. The iron-dependent degradation of $IRP1_{C437S}$ involved ubiquitination, required ongoing transcription and translation, and could be efficiently blocked by the proteasomal inhibitors MG132 and lactacystin. Similar results were obtained with overexpressed wild-type IRP1, which predominated in the apo-form even in iron-loaded H1299 cells, possibly due to saturation of the ISC assembly machinery. Importantly, inhibition of ISC biogenesis in HeLa cells by small interfering RNA knockdown of the cysteine desulfurase Nfs1 sensitized endogenous IRP1 for iron-dependent degradation. Collectively, these data uncover a mechanism for the regulation of IRP1 abundance as a means to control its RNA-binding activity, when the ISC assembly pathway is impaired.

Iron regulatory proteins IRP1 and IRP2 are cytoplasmic posttranscriptional regulators of cellular iron metabolism (26, 31). They bind with high affinity to "iron-responsive elements" (IREs), stem-loop structures in the untranslated regions of several mRNAs, such as those encoding transferrin receptor 1 (TfR1), H- and L-ferritin, ferroportin, erythroid aminolevulinate synthase, and mitochondrial aconitase. IRE/IRP interactions control the stability of TfR1 mRNA and the translation of the other mRNAs, thereby promoting homeostatic responses to iron deficiency.

IRP1 and IRP2 are ubiquitously expressed in tissues and appear to have at least partially redundant functions. Thus, mice with single IRP1 (11, 22) or IRP2 (5, 12) deficiency are viable, while double $IRP1^{-/-}$ $IRP2^{-/-}$ knockout mice exhibit early embryonic lethality (35). The ablation of IRP1 yielded a mild phenotype with minor misregulation of iron metabolism in the kidney and brown fat (22). The targeted disruption of IRP2 resulted in microcytosis (5, 12) and has been associated with a neurodegenerative movement disorder (19, 34); nevertheless, $IRP2^{-/-}$ mice without neurological defects have also been reported (13).

IRP1 and IRP2 share considerable homology with mitochondrial aconitase and belong to the iron-sulfur cluster (ISC) isomerase family (10), but they are regulated by diverse mechanisms. Thus, in iron-replete cells, IRP2 undergoes degradation by the proteasome, while IRP1 assembles a cubane [4Fe-4S] cluster that prevents IRE binding (26, 31). The ISC coordinates at C437, C503, and C506 (6) and converts IRP1 to a cytosolic aconitase. The reversible switch between holo- and apo-IRP1 is associated with conformational changes (2, 43). The mechanism for ISC assembly in IRP1 is incompletely characterized and very likely involves a large set of mitochondrial and cytoplasmic components, including frataxin (21, 33, 36), glutaredoxin 5 (42), Abcb7 (30), Nfs1 (1), Isu1 (38), and Cfd1 (32).

An IRP1 mutant with a phosphomimetic S138E substitution, which is defective in maintaining an ISC under aerobic conditions (3), undergoes degradation in iron-replete cells (4, 8). This finding provided the first link between the status of the ISC and protein stability. Here, we further investigate the effects of iron in the stability of IRP1 and show that, under conditions where ISC biogenesis is impaired, apo-IRP1 is sensitized for iron-dependent degradation via the ubiquitin-proteasome pathway.

MATERIALS AND METHODS

Materials. Hemin, ferric ammonium citrate (FAC), MG132, lactacystin, bafilomycin A1, cycloheximide, and actinomycin D were purchased from Sigma (St. Louis, MI). Desferrioxamine (DFO) was from Novartis (Dorval, Canada).

Cell culture. Human H1299 (lung cancer) and HeLa (cervix carcinoma) cells were grown in Dulbecco's modified Eagle medium supplemented with 10% fetal bovine serum, 2 mM glutamine, 100 U/ml penicillin, and 0.1 mg/ml streptomycin. H1299 clones expressing either $IRP1_{C437S}$ ($HIRP1_{mut}$) or wild-type IRP1 ($HIRP1_{wt}$) by a tetracycline-dependent promoter (tet-off system) were main-

* Corresponding author. Mailing address: Lady Davis Institute for Medical Research, Sir Mortimer B. Davis Jewish General Hospital, 3755 Cote-Ste-Catherine Road, Montreal, Quebec H3T 1E2, Canada. Phone: (514) 340-8260, ext. 5293. Fax: (514) 340-7502. E-mail: kostas.pantopoulos@mcgill.ca.

¶ Present address: Department of Biochemistry, University of Texas Southwestern Medical Center, Dallas, TX.

Present address: Department of Physiology, University of Texas Southwestern Medical Center, Dallas, TX.

† These authors equally contributed to the work.

▽ Published ahead of print on 22 January 2007.

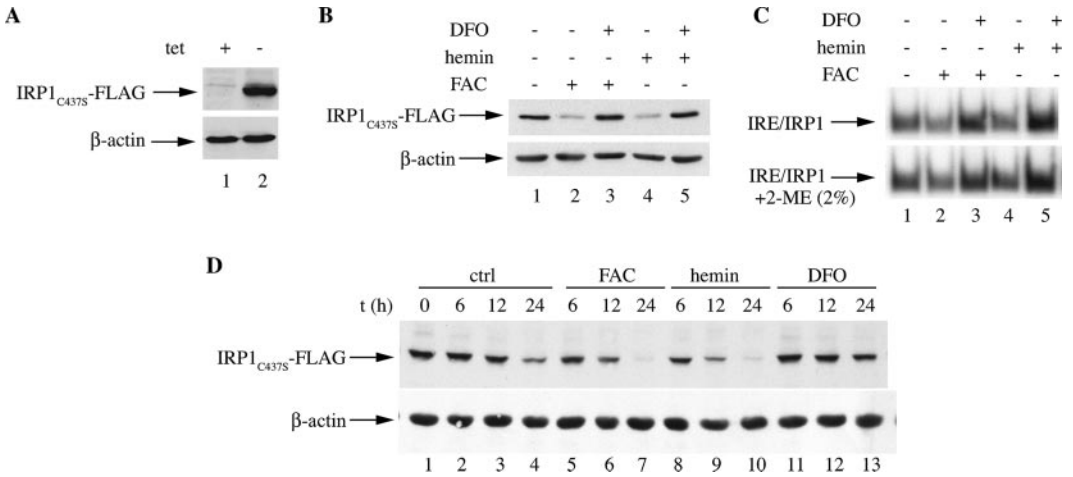

FIG. 1. Iron-dependent degradation of $IRP1_{C437S}$. (A) $HIRP1_{mut}$ cells were grown for 48 h in the absence (−) or presence (+) of 2 μg/ml tetracycline (tet). The expression of transfected FLAG-tagged $IRP1_{C437S}$ was analyzed by immunoblotting; the blots were hybridized with FLAG (top) and control β-actin (bottom) antibodies. (B to D) $HIRP1_{mut}$ cells were grown without tetracycline to accumulate $IRP1_{C437S}$. After 48 h, tetracycline was added back in the media and the cells were exposed overnight (B and C), or for the indicated time intervals (D), to 30 μg/ml FAC, 100 μM hemin, or 100 μM DFO (no addition is marked by "ctrl"). The expression of $IRP1_{C437S}$ (top) and control β-actin (bottom) was analyzed by immunoblotting (B and D). IRE-binding activity was analyzed by EMSA with a ^{32}P-labeled IRE probe in the absence (top) or presence (bottom) of 2% 2-mercaptoethanol (2-ME); IRE/IRP1 complexes are indicated by arrows (C).

tained in the presence of 2 μg/ml tetracycline, 2 μg/ml puromycin, and 250 μg/ml G418. The $HIRP1_{wt}$ cells were generated with the same approach employed earlier for $HIRP1_{mut}$ cells (41). 293-GPG packaging cells (25) were grown in supplemented Dulbecco's modified Eagle medium in the presence of 1 μg/ml tetracycline, 2 μg/ml puromycin, and 300 μg/ml G418.

Immunoblotting. Cells were washed twice in phosphate-buffered saline (PBS) and lysed in cytoplasmic lysis buffer (25 mM Tris-Cl, pH 7.4, 40 mM KCl, and 1% Triton X-100). Cell debris was cleared by centrifugation, and the protein concentration was determined with the Bradford reagent (Bio-Rad). Cell lysates (30 μg) or, when indicated, immunoprecipitated material were resolved by sodium dodecyl sulfate-polyacrylamide gel electrophoresis (SDS-PAGE) on 8% gels, and the proteins were transferred onto nitrocellulose filters. The blots were saturated with 10% nonfat milk in PBS and probed with FLAG (M2-FLAG; Sigma), IRP1 (8), IRP2 (12), Nfs1 (1), β-actin (Sigma), or ubiquitin (Santa Cruz) antibodies, diluted 1:1,000 in PBS containing 5% nonfat milk and 0.5% Tween 20 (PBST). Following the wash with PBST, the blots with monoclonal FLAG and ubiquitin antibodies were incubated with peroxidase-coupled rabbit anti-mouse immunoglobulin G (1:4,000 dilution). The blots with polyclonal β-actin antibodies were incubated with peroxidase-coupled goat anti-rabbit immunoglobulin G (1:5,000 dilution). Detection was performed with the enhanced chemiluminescence method (Amersham). The immunoreactive bands were quantified by densitometric scanning.

Pulse-chase and immunoprecipitation. Cells were metabolically labeled for 2 h with 50 μCi/ml trans-^{35}S-label, a mixture of 70:30 [^{35}S]methionine/cysteine (ICN). The radioactive medium was then removed, and the cells were chased in cold media. The chase was terminated by a wash in PBS. The cells were lysed in a buffer containing 1% Triton X-100, 50 mM Tris-Cl, pH 7.4, and 300 mM NaCl. Cell debris was cleared by centrifugation, and cell lysates were subjected to quantitative immunoprecipitation with the FLAG antibody (8.8 μg antibody was used for 500 μg lysates, representing an equal number of cells). Immunoprecipitated proteins were analyzed by SDS-PAGE. Radioactive bands were visualized by autoradiography and quantified by phosphorimaging.

Electrophoretic mobility shift assay (EMSA). Cells were lysed in cytoplasmic lysis buffer. Cytoplasmic lysates were analyzed for IRE-binding activity by an electrophoretic mobility shift assay with a ^{32}P-labeled IRE probe (23).

RNA interference. A pSUPERretro vector-based approach was employed to knock down Nfs1 with gene-specific targeting sequences corresponding to positions 1040 to 1059 (GCACCATTATCCCGGCTGT; huNFS1-R3) of its coding region (1). Forward and reverse oligonucleotides were annealed and cloned into the BglII-HindIII restriction sites of the vector. Control pSUPERretro and pSUPERretro-Nfs1 vectors were transiently transfected, by using the Lipofectamine reagent (Invitrogen), into 293-GPG packaging cells (kindly provided by J. Galipeau, McGill University) to produce vesicular stomatitis virus G protein (VSVG)-pseudotyped retroviral supernatants. After 48 h, conditioned media were passed through a 0.45-μm filter and utilized for infection (six times with 12-h intervals) of HeLa cells in the presence of 8 μg/ml Polybrene (Sigma). Puromycin-resistant, stably transduced cells were selected and expanded, and the expression of Nfs1 was monitored by immunoblotting.

Aconitase assay. Cells were lysed either with cytoplasmic lysis buffer or with digitonin (to prepare pure cytosolic extracts devoid of mitochondrial contamination) (14). Aconitase activity in crude or pure cytosolic extracts was measured by the reduction of $NADP^+$ at 340 nm in a coupled reaction with isocitrate dehydrogenase, in the presence of 200 μM citrate as substrate (7, 14). One unit of aconitase was defined as the amount that converts 1 μmol of substrate per minute at pH 7.4 and 25°C. The activity was always normalized to the total amount of protein in the extracts.

Statistical analysis. Data are shown as means ± standard deviations (SD). Statistical analysis was performed by either the unpaired Student's *t* test or the one-way analysis of variance test with the Prism GraphPad software (version 4.0c).

RESULTS

The constitutive $IRP1_{C437S}$ mutant is sensitive to iron-dependent degradation by the proteasome. Because C437 is critical for ISC coordination, IRP1 bearing a C437S point mutation remains an apo-protein and displays constitutive IRE-binding activity (17, 29). We previously developed H1299 cells expressing functional FLAG-tagged $IRP1_{C437S}$ by a tetracycline-dependent promoter ($HIRP1_{mut}$ cells) (41). The removal of tetracycline from the media results in robust expression of $IRP1_{C437S}$ (Fig. 1A). Readdition of tetracycline inhibits de novo synthesis of the protein and allows studies on its stability. Under these conditions, we noticed that an overnight treatment of cells with iron, either in the form of FAC or hemin, drastically decreased the expression (Fig. 1B) and the IRE-binding activity (Fig. 1C) of $IRP1_{C437S}$. These responses were completely blocked by the iron chelator DFO (lanes 3 and 5 in Fig. 1B and C). In a time course experiment, iron destabilized $IRP1_{C437S}$ within 12 h and promoted its complete degradation after 24 h (Fig. 1D). None of the manipulations

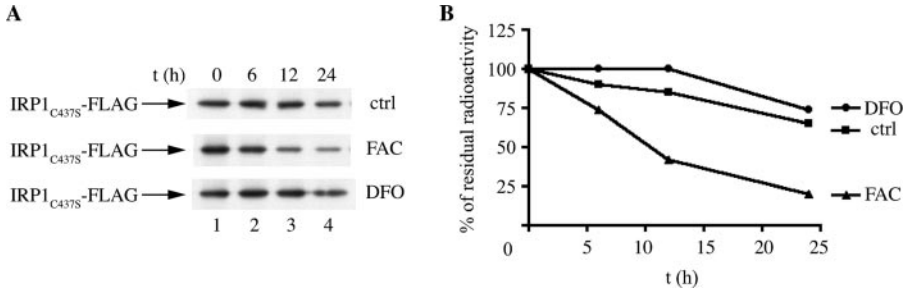

FIG. 2. Iron accelerates the turnover of $IRP1_{C437S}$. $HIRP1_{mut}$ cells grown for 48 h in tetracycline-free media were metabolically labeled for 2 h with [^{35}S]methionine/cysteine and chased with cold media for the indicated time intervals without any iron perturbations (ctrl), or in the presence of 30 μg/ml FAC or 100 μM DFO. The decay of $IRP1_{C437S}$ was assessed by quantitative immunoprecipitation. (A) Immunoprecipitated material was analyzed by SDS-PAGE on 8% gels, and proteins were visualized by autoradiography. (B) Radioactive bands were quantified by phosphorimaging and plotted against the time.

altered the levels of endogenous β-actin (bottom panels of Fig. 1A, B, and D).

The effects of iron on $IRP1_{C437S}$ stability were directly assessed by a pulse-chase experiment (Fig. 2). $HIRP1_{mut}$ cells were metabolically labeled with [^{35}S]methionine/cysteine for 2 h. Subsequently, the cells were subjected to iron perturbations during a chase for 6 to 24 h, and the decay of $IRP1_{C437S}$ was monitored by immunoprecipitation with the FLAG antibody (Fig. 2A). In the presence of FAC during the chase, the half-life of $IRP1_{C437S}$ was reduced from ~24 h to ~10 h (Fig. 2B). Taken together, these results demonstrate that $IRP1_{C437S}$ is sensitive to degradation in the presence of high concentrations of heme or nonheme iron.

To gain mechanistic insights, we examined the potential of various drugs to interfere with the degradation pathway (Fig. 3). Actinomycin D and cycloheximide, which are established inhibitors of mRNA transcription and translation, respectively, efficiently antagonized $IRP1_{C437S}$ turnover in response to FAC or hemin (Fig. 3A) without affecting $IRP1_{C437S}$ expression in the absence of iron sources (data not shown). This indicates that active protein synthesis is required for the iron-dependent degradation to occur. While ammonium chloride and bafilomycin A1, which block protein degradation in lysosomes, did not have any appreciable effect on $IRP1_{C437S}$ stability, the proteasomal inhibitors MG132 and lactacystin abolished $IRP1_{C437S}$ degradation in cells exposed to FAC (Fig. 3B). Importantly, the arrest of the degradation pathway by MG132 was associated with the accumulation of polyubiquitinated $IRP1_{C437S}$ species (Fig. 3C, upper panel). The lack of signal in extracts of tetracycline-treated cells (lanes 1 to 4) underlies the specificity of this response. The absence of tetracycline throughout the experiment (lanes 5 to 8) allowed continuous expression of $IRP1_{C437S}$; under these conditions, the steady-state levels of $IRP1_{C437S}$ were not affected by the iron treat-

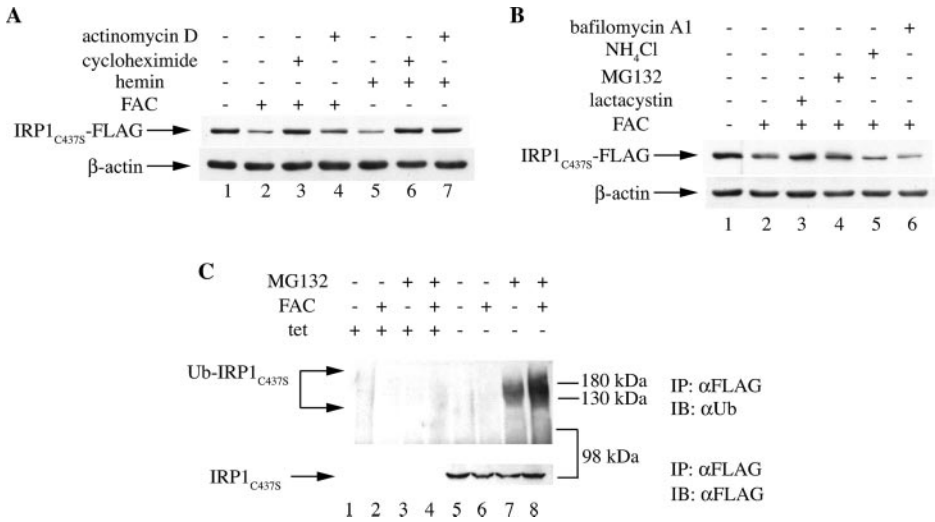

FIG. 3. Iron-dependent degradation of $IRP1_{C437S}$ is mediated by the proteasome. (A and B) $HIRP1_{mut}$ cells were grown without tetracycline to accumulate $IRP1_{C437S}$. After 48 h, tetracycline (2 μg/ml) was added back to the media and the cells were treated for 24 h with the indicated drugs (5 μM actinomycin D, 40 μM cycloheximide, 100 μM hemin, 30 μg/ml FAC, 100 nM bafilomycin A1, 25 mM NH_4Cl, 10 μM MG132, or 10 μM lactacystin). The expression of $IRP1_{C437S}$ (top) and control β-actin (bottom) was analyzed by immunoblotting. (C) $HIRP1_{mut}$ cells were grown for 48 h in the absence (−) or presence (+) of 2 μg/ml tetracycline (tet) and left untreated or treated overnight with 30 μg/ml FAC and/or 10 μM MG132. Cell lysates were prepared and subjected to quantitative immunoprecipitation (IP) with the FLAG antibody. Immunoprecipitated material was analyzed by immunoblotting (IB). The blots were hybridized with antibodies against ubiquitin (Ub; top) or FLAG (bottom). The antibodies utilized for immunoprecipitation and immunoblotting are also indicated on the right of each panel.

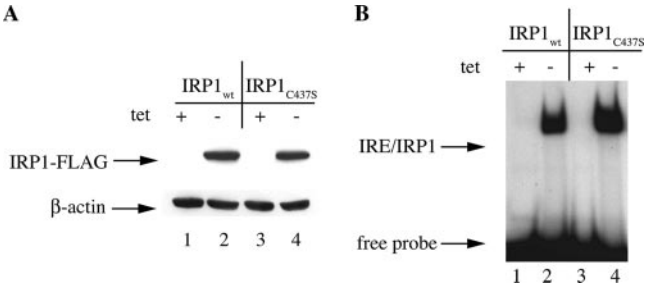

FIG. 4. Tetracycline-dependent expression and IRE-binding activity of $IRP1_{wt}$. $HIRP1_{wt}$ and $HIRP1_{mut}$ cells were grown for 48 h in the absence (−) or presence (+) of 2 μg/ml tetracycline (tet). (A) The expression of transfected FLAG-tagged $IRP1_{wt}$ and $IRP1_{C437S}$ was analyzed by immunoblotting; the blots were hybridized with FLAG (top) and control β-actin (bottom) antibodies. (B) IRE-binding activity was analyzed by EMSA with a ^{32}P-labeled IRE probe; IRE/IRP1 complexes and excess free probe are indicated by arrows.

ment (Fig. 3C, bottom panel). In conclusion, the data in Fig. 3 suggest that the iron-dependent degradation of $IRP1_{C437S}$ requires active protein synthesis, proceeds via the proteasome, and involves ubiquitination of the protein.

Tetracycline-dependent expression of $IRP1_{wt}$. H1299 cells were engineered for tetracycline-dependent expression of wild-type IRP1 ($HIRP1_{wt}$ cells). Removal of tetracycline from the media derepressed the expression of FLAG-tagged $IRP1_{wt}$ in $HIRP1_{wt}$ cells at levels comparable to those of $IRP1_{C437S}$ in $HIRP1_{mut}$ cells (Fig. 4A). The accumulation of transfected $IRP1_{wt}$ was associated with a dramatic increase in IRE-binding activity (Fig. 4B, lanes 1 to 2). This was likewise comparable to the activity of transfected $IRP1_{C437S}$ in $HIRP1_{mut}$ cells (Fig. 4B, compare lanes 2 and 4), previously estimated to represent a ~100-fold increase over the activity of endogenous IRP1 (41).

A treatment of $HIRP1_{wt}$ cells with FAC for 12 h resulted in a ~15% decrease in the IRE binding (Fig. 5A) and a concomitant ~15% increase in aconitase activity (Fig. 5B) of $IRP1_{wt}$, without affecting its steady-state levels (Fig. 5C). To calculate the alterations in aconitase, endogenous activity unrelated to $IRP1_{wt}$ expression (Fig. 5B, +tet) was subtracted. The ratios of IRE-binding or aconitase activities of $IRP1_{wt}$ with its mass define the relative distribution of the protein between the [4Fe-4S]- and the apo-forms. These calculations reveal that in the absence of an exogenous iron source, the vast majority (~80%) of $IRP1_{wt}$ was expressed as an apo-protein and only ~20% assembled an ISC (Fig. 5D). The addition of FAC expanded the pool of [4Fe-4S]-$IRP1_{wt}$ by ~15% (Fig. 5D) but failed to promote a complete ISC switch, suggesting that iron was only partially limiting for full-scale ISC assembly. Similar results were obtained with at least three additional clones of H1299 cells expressing high levels of $IRP1_{wt}$ (data not shown).

Iron-mediated proteasomal degradation of transfected wild-type apo-IRP1. Having established that overexpressed $IRP1_{wt}$ predominates in the apo-form, we evaluated whether iron affects its stability in a time course experiment (Fig. 6A). Exposure of cells to FAC or hemin destabilized $IRP1_{wt}$ within 12 to 24 h (compare lane 1 with lanes 6 to 7 and 9 to 10, top panel), while levels of control β-actin remained unaltered (bottom

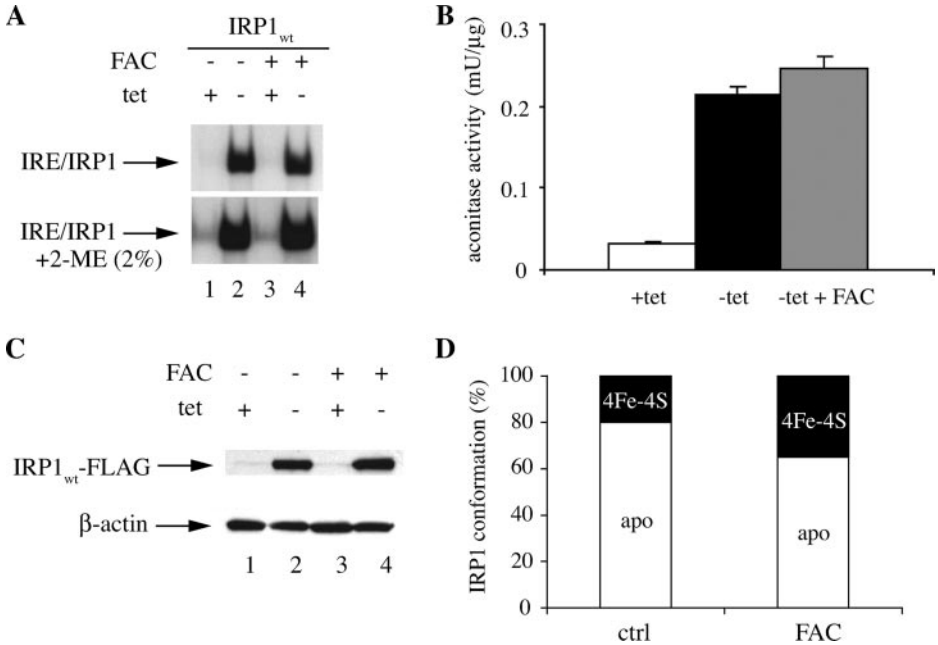

FIG. 5. $IRP1_{wt}$ is predominantly expressed as an apo-protein. $HIRP1_{wt}$ cells were grown for 48 h with (+) or without (−) tetracycline. Subsequently, tetracycline (tet; 2 μg/ml) was added back, $HIRP1_{wt}$ cells were further incubated for 12 h in the absence or presence of 30 μg/ml FAC, and pure cytoplasmic lysates were prepared. (A) IRE-binding activity was analyzed by EMSA with a ^{32}P-labeled IRE probe in the absence (top) or presence (bottom) of 2% 2-mercaptoethanol (2-ME); IRE/IRP1 complexes are indicated by arrows. (B) Aconitase activity, corresponding to mean ± SD values from triplicate samples. (C) The expression of $IRP1_{wt}$ was analyzed by immunoblotting; the blots were hybridized with FLAG (top) and control β-actin (bottom) antibodies. (D) Quantification of the relative distribution of $IRP1_{wt}$ between the [4Fe-4S]- and apo-forms. Values correspond to the ratios of IRE binding and aconitase activities to the mass of the protein.

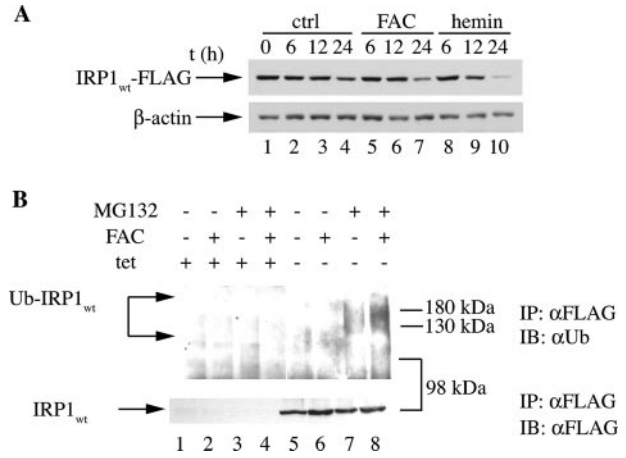

FIG. 6. Iron-dependent degradation of $IRP1_{wt}$ by the proteasome. (A) $HIRP1_{wt}$ cells were grown without tetracycline to accumulate FLAG-tagged $IRP1_{wt}$. After 48 h, tetracycline (2 μg/ml) was added back in the media and the cells were exposed for the indicated time intervals to 30 μg/ml FAC or 100 μM hemin (no addition is marked by "ctrl"). The expression of FLAG-tagged $IRP1_{wt}$ (top) and control β-actin (bottom) was analyzed by immunoblotting. (B) $HIRP1_{wt}$ cells were grown for 48 h in the absence (−) or presence (+) of 2 μg/ml tetracycline (tet) and left untreated or treated overnight with 30 μg/ml FAC and/or 10 μM MG132. Cell lysates were prepared and subjected to quantitative immunoprecipitation (IP) with the FLAG antibody. Immunoprecipitated material was analyzed by immunoblotting (IB). The blots were hybridized with antibodies against ubiquitin (Ub; top) or FLAG (bottom). The antibodies utilized for immunoprecipitation and immunoblotting are also indicated on the right of each panel.

panel). Importantly, FAC promoted the ubiquitination of $IRP1_{wt}$ (Fig. 6B), by analogy to $IRP1_{C437S}$ (shown in Fig. 3C). In conclusion, these results suggest that iron triggers the degradation of apo-IRP1 by the proteasome.

Partial depletion of mitochondrial Nfs1 inhibits ISC assembly and sensitizes endogenous IRP1 to iron-dependent degradation. To investigate the biological relevance of the above findings, we established conditions for inhibition of ISC formation in endogenous IRP1. A small interfering RNA (siRNA) approach was designed to knock down the cysteine desulfurase Nfs1, which catalyzes an essential step in ISC biogenesis of mitochondrial proteins (20) but also of cytosolic IRP1 (1). HeLa cells were infected with VSVG-pseudotyped retroviral particles containing pSUPERretro-Nfs1 to target Nfs1, or control empty vector. Two weeks postinfection, stably transduced cells were selected and the content of Nfs1 was monitored by immunoblotting. The siRNA targeting reduced the expression of Nfs1 by ~85% (Fig. 7A). This was associated with a ~4-fold induction in IRE binding (Fig. 7B and C) and a ~30% decrease in aconitase activity (Fig. 7D), consistent with recent observations showing Nfs1-related defects in the activity of ISC-proteins (1, 9). Notably, while the complete elimination of Nfs1 severely inhibited growth of HeLa cells (1), the stably transduced HeLa cells with ~15% residual expression of this protein did not exhibit any growth defects (Fig. 7E). We conclude that the partial depletion of Nfs1 promotes a shift in the pool of cellular IRP1 from the [4Fe-4S]- to the apo-form, apparently due to inhibition of the ISC assembly pathway.

To examine the effects of iron on the stability of apo-IRP1, control and Nfs1-deficient HeLa cells were exposed overnight

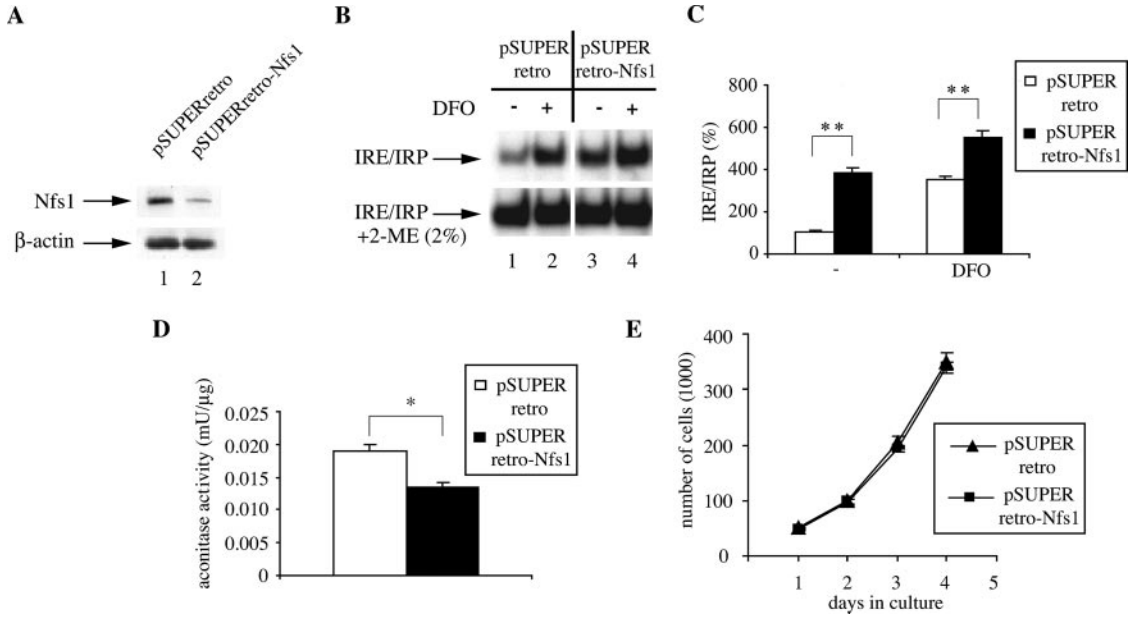

FIG. 7. Partial depletion of Nfs1 activates endogenous IRP1 for IRE binding. HeLa cells were infected with VSVG-pseudotyped retroviral particles containing pSUPERretro-Nfs1 or empty pSUPERretro vector. (A) Two weeks postinfection, the expression of mitochondrial Nfs1 (top) and β-actin (bottom) was examined by immunoblotting. (B) Transduced cells were left untreated or exposed overnight to 100 μM DFO, and IRE-binding activity was analyzed by EMSA with a ^{32}P-labeled IRE probe in the absence (top) or presence (bottom) of 2% 2-mercaptoethanol (2-ME). IRE/IRP complexes are indicated by arrows. (C) IRE/IRP band intensities from three independent experiments (means ± SD) were quantified by phosphorimaging and plotted on the right, following normalization with the respective values obtained with 2-mercaptoethanol. (D) Crude cytoplasmic lysates were analyzed for aconitase activity; values correspond to means ± SD from triplicate samples. (E) The growth rate of transduced cells was monitored by direct cell counting. Similar results were obtained with the 3-(4,5-dimethylthiazol-2-yl)-2,5-diphenyltetrazolium bromide proliferation assay (data not shown). *, $P < 0.05$; **, $P < 0.01$ (Student's t test).

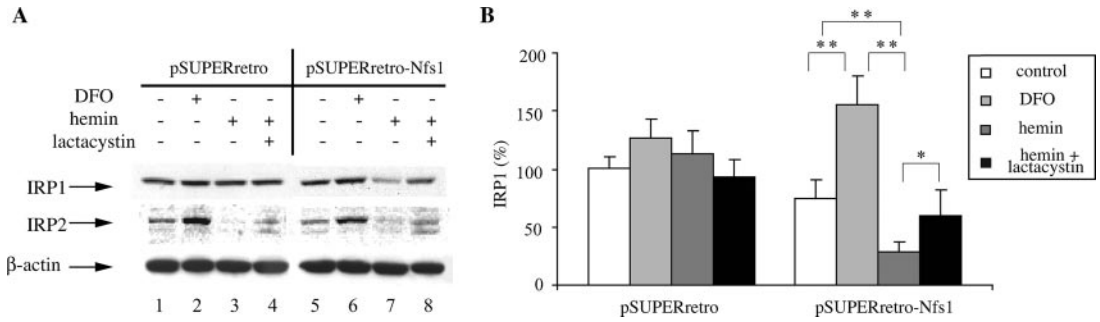

FIG. 8. Iron-dependent degradation of endogenous IRP1 in Nfs1-deficient cells. (A) HeLa cells transduced with pSUPERretro or pSUPERretro-Nfs1, respectively, for two weeks, were either left untreated or exposed overnight to 100 μM DFO or 100 μM hemin, in the absence or presence of 10 μM lactacystin. Cell lysates were prepared and analyzed by immunoblotting for expression of IRP1 (top), IRP2 (middle), and β-actin (bottom). (B) The data from three independent experiments were quantified by densitometry, and relative IRP1 band intensities (means ± SD) were normalized with the respective β-actin values and plotted on the right. *, $P < 0.05$; **, $P < 0.01$ (one-way analysis of variance test).

to DFO or hemin. In control cells, IRP1 expression was largely unresponsive to iron perturbations (Fig. 8A, top panel, and B). However, in Nfs1-deficient cells, DFO appeared to stabilize IRP1, while hemin decreased IRP1 levels by a lactacystin-sensitive mechanism. As expected, IRP2 was induced by DFO and destabilized by hemin in a similar fashion in both control and Nfs1-deficient HeLa cells (Fig. 8A, middle panel), while the expression of control β-actin remained unaffected (Fig. 8A, bottom panel). Taken together, these results suggest that, under conditions where ISC biogenesis is impaired, endogenous apo-IRP1 is sensitized for iron-dependent proteasomal degradation.

DISCUSSION

IRP1 is primarily regulated by an unusual posttranslational mechanism involving a reversible ISC switch (26, 31). Thus, in iron-depleted cells, IRP1 predominates as an apo-protein and exhibits IRE-binding activity. In iron-replete cells, the IRE-binding activity is abolished by the assembly of an ISC and IRP1 acquires enzymatic activity as cytosolic aconitase. Earlier reports also established that IRP1 is a relatively stable protein, with a half-life of >12 h that is not affected by iron (27, 37), in sharp contrast to IRP2, which undergoes rapid iron-dependent degradation by the proteasome (15).

We have shown that IRP1 bearing a phosphomimetic S138E substitution is sensitive to iron-mediated degradation that can be blocked by proteasomal inhibitors (8). Importantly, the conserved S138 is located in close proximity to the aconitase active site cleft (6) and its replacement with a negatively charged glutamate residue compromises the stability of the ISC under aerobic conditions (3, 8). Even though these data were obtained with a nonphysiological mutant, they have raised the intriguing possibility for an additional mode of IRP1 regulation besides the established ISC switch, at the level of protein stability.

Here, we first utilized $IRP1_{C437S}$, an IRP1 variant exhibiting a more direct defect in ISC formation, due to the replacement of crucial C437, that anchors the [4Fe-4S] cluster (6). We demonstrate that exposure of $HIRP1_{mut}$ cells to heme or non-heme iron destabilized $IRP1_{C437S}$ (Fig. 1) and accelerated its degradation (Fig. 2). This was antagonized by actinomycin D and cycloheximide (Fig. 3A), suggesting that the iron-mediated degradation of $IRP1_{C437S}$ requires ongoing transcription and apparently depends on the synthesis of independent protein(s), by analogy to IRP2 (16, 40). The inhibitory effects of MG132 and lactacystin (Fig. 3B) implicate the proteasome in the degradation pathway. Moreover, the mechanism involves ubiquitination of $IRP1_{C437S}$ (Fig. 3C).

Interestingly, similar results were obtained with $HIRP1_{wt}$ cells, expressing wild-type IRP1 under the tight control of a tetracycline-dependent promoter. Both $IRP1_{C437S}$ and $IRP1_{wt}$ were expressed at high levels (Fig. 4A) and exhibited profound IRE-binding activities (Fig. 4B). $IRP1_{wt}$ predominated in the apo-form, even after treatment with FAC, which merely promoted a partial assembly of its ISC (Fig. 5). Note that iron supplementation was sufficient to drastically reduce the IRE-binding activity of endogenous IRP1 in various cell lines (16, 24, 28), which is indicative of an efficient ISC switch. Our data suggest that the apparently low efficiency of $IRP1_{wt}$ to assemble an ISC is only partially due to the unavailability of iron. We speculate that this response may be related to a saturation of the ISC assembly machinery due to overexpression of the substrate rather than reflecting an inherent incompetence of exogenously transfected IRP1 in ISC biogenesis. In support of this notion, previous experiments revealed that exogenous $IRP1_{wt}$ possesses robust aconitase activity when transfected in B6 fibroblasts (7, 8, 18) or HEK293 cells (4).

Figure 6 demonstrates that, similar to $IRP1_{C437S}$, overexpressed $IRP1_{wt}$ undergoes degradation in iron-loaded cells, by a mechanism that involves ubiquitination. $IRP1_{wt}$ appears relatively more resistant than $IRP1_{C437S}$ following iron treatments (compare Fig. 6A with 1D), consistent with partial ISC assembly that stabilizes the protein. It should be noted that the kinetics for iron-dependent degradation of IRP1, in the form of either $IRP1_{wt}$ (Fig. 6A), $IRP1_{C437S}$ (Fig. 1D and 2), or $IRP1_{S138E}$ (8), are substantially slower than the degradation of IRP2 in response to iron (15, 39). Experiments are under way to identify and characterize sequences within IRP1 and IRP2 that account for these differences.

The data in Fig. 1 to 6 establish a link between the stability of IRP1 and the status of its ISC. This is further substantiated by the sensitization of endogenous apo-IRP1 for iron-dependent degradation in HeLa cells partially depleted from the cysteine desulfurase Nfs1 (Fig. 7 to 8), an essential factor for

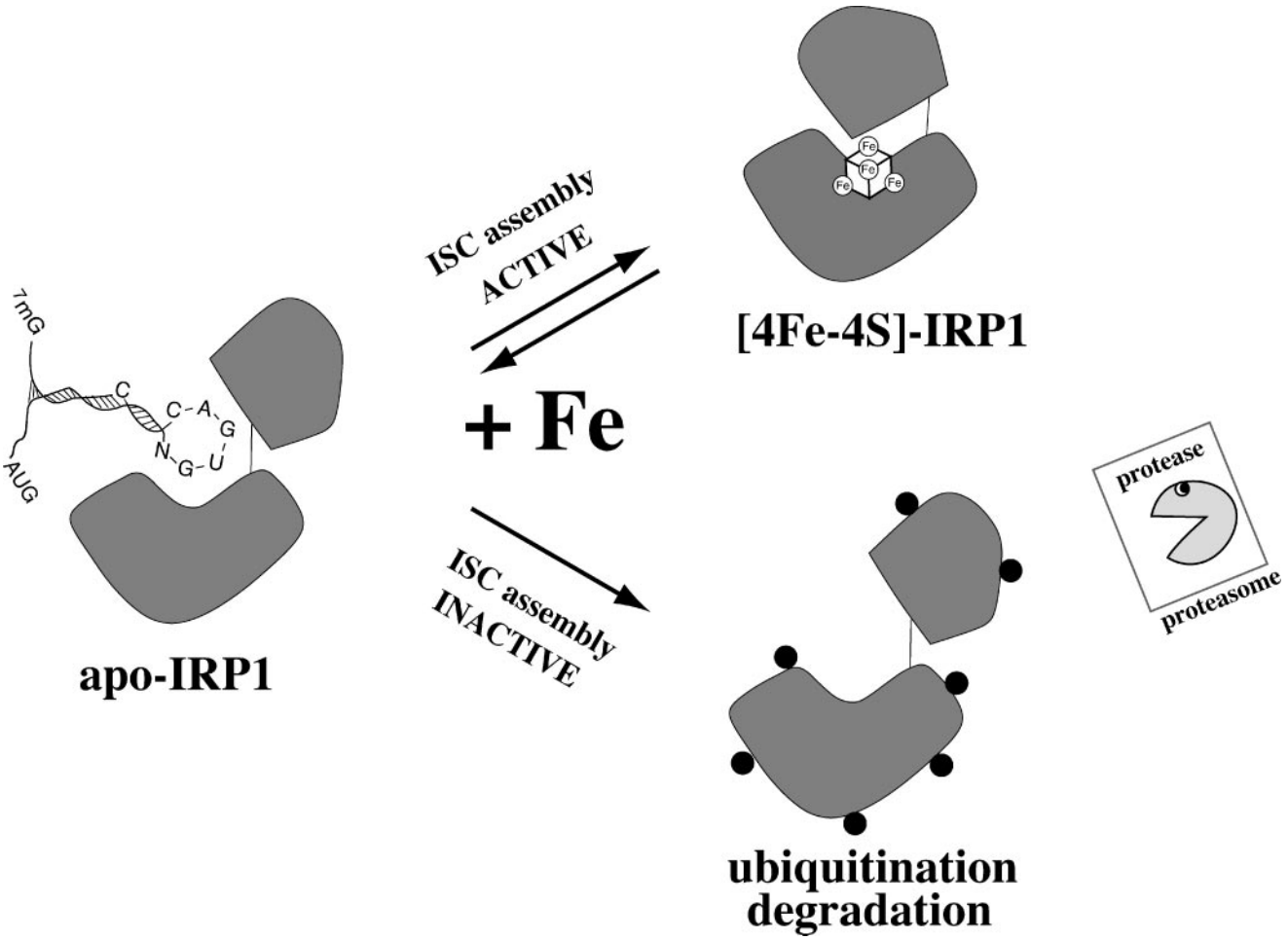

FIG. 9. A model for the regulation of IRP1. In iron-deficient cells, IRP1 is present as an apo-protein, which is active in IRE binding (left part). An increase in cellular iron levels results in reversible assembly of a cubane [4Fe-4S] cluster that converts it to cytosolic aconitase. Under conditions where the ISC assembly pathway is not functional, IRP1 is sensitized for iron-dependent degradation by the ubiquitin-proteasome pathway.

ISC biogenesis (20). Likewise, the siRNA-mediated depletion of Nfs1 in NIH 3T3 cells decreased IRP1 content without affecting the levels of xanthine oxidase, an unrelated ISC-containing protein (9). These results are also consistent with the decreased abundance of IRP1 in iron-rich livers from $Sod^{-/-}$ and $Abcb7^{-/-}$ mice, which display defects in ISC maintenance and assembly, respectively (4).

It is noteworthy that the depletion of Nfs1 activated IRP1 for IRE binding (Fig. 6; also see references 1 and 9), suggesting that this protein is also functional in cytosolic ISC biogenesis. Because IRE/IRP1 and IRE/IRP2 complexes from human cell extracts comigrate in gel shift assays, it is formally possible that IRP2 may also contribute to the increase in total IRE-binding activity shown in Fig. 7. However, the knockdown of Nfs1 did not affect the expression of IRP2 (Fig. 8A). Along these lines, the disruption of ISC biogenesis by siRNA-mediated suppression of the scaffold protein Isu1 in HeLa cells not only activated IRP1 for IRE binding but also induced IRP2 expression (38). It is conceivable that further elimination of the residual (~15%) Nfs1 expression may trigger IRP2 responses, similar to those observed in Isu1-depleted cells.

In summary, we describe a mechanism for IRP1 regulation at the level of protein stability, which complements the "classical" ISC switch and, moreover, couples ISC biochemistry with protein turnover. We propose that the ISC not only converts IRP1 into a cytosolic aconitase but also stabilizes the protein against proteolysis. The model illustrated in Fig. 9 postulates that under conditions where IRP1 fails to assemble an ISC in response to increased cellular iron levels, excess IRE-binding activity is irreversibly controlled by protein degradation via the ubiquitin-proteasome pathway. Physiological conditions favoring the operation of this alternative mechanism remain to be identified.

ACKNOWLEDGMENTS

This paper is dedicated to the memory of Spyros Karakalas.

The work was supported by a grant from the Canadian Institutes for Health Research. J.W. was the recipient of a fellowship from the Fonds de la recherche en santé du Quebéc (FRSQ). K.P. holds a senior career award from FRSQ. R.L. acknowledges support from Sonderforschungsbereiche 593 and TR1, Deutsche Forschungsgemeinschaft (Gottfried-Wilhelm Leibniz program and GRK1216), and Fonds der chemischen Industrie.

REFERENCES

1. **Biederbick, A., O. Stehling, R. Rösser, B. Niggemeyer, Y. Nakai, H. P. Elsässer, and R. Lill.** 2006. Role of human mitochondrial Nfs1 in cytosolic iron-sulfur protein biogenesis and iron regulation. Mol. Cell. Biol. **26:**5675–5687.
2. **Brazzolotto, X., P. Timmins, Y. Dupont, and J. M. Moulis.** 2002. Structural changes associated with switching activities of the human iron regulatory protein 1. J. Biol. Chem. **277:**11995–12000.
3. **Brown, N. M., S. A. Anderson, D. W. Steffen, T. B. Carpenter, M. C. Kennedy, W. E. Walden, and R. S. Eisenstein.** 1998. Novel role of phosphorylation in Fe-S cluster stability revealed by phosphomimetic mutations at Ser-138 of iron regulatory protein 1. Proc. Natl. Acad. Sci. USA **95:**15235–15240.
4. **Clarke, S. L., A. Vasanthakumar, S. A. Anderson, C. Pondarre, C. M. Koh, K. M. Deck, J. S. Pitula, C. J. Epstein, M. D. Fleming, and R. S. Eisenstein.** 2006. Iron-responsive degradation of iron-regulatory protein 1 does not require the Fe-S cluster. EMBO J. **25:**544–553.
5. **Cooperman, S. S., E. G. Meyron-Holtz, H. Olivierre-Wilson, M. C. Ghosh, J. P. McConnell, and T. A. Rouault.** 2005. Microcytic anemia, erythropoietic protoporphyria and neurodegeneration in mice with targeted deletion of iron regulatory protein 2. Blood **106:**1084–1091.
6. **Dupuy, J., A. Volbeda, P. Carpentier, C. Darnault, J. M. Moulis, and J. C. Fontecilla-Camps.** 2006. Crystal structure of human iron regulatory protein 1 as cytosolic aconitase. Structure **14:**129–139.
7. **Fillebeen, C., A. Caltagirone, A. Martelli, J. M. Moulis, and K. Pantopoulos.** 2005. IRP1 Ser-711 is a phosphorylation site, critical for regulation of RNA-binding and aconitase activities. Biochem. J. **388:**143–150.
8. **Fillebeen, C., D. Chahine, A. Caltagirone, P. Segal, and K. Pantopoulos.** 2003. A phosphomimetic mutation at Ser-138 renders iron regulatory protein 1 sensitive to iron-dependent degradation. Mol. Cell. Biol. **23:**6973–6981.
9. **Fosset, C., M. J. Chauveau, B. Guillon, F. Canal, J. C. Drapier, and C. Bouton.** 2006. RNA silencing of mitochondrial m-Nfs1 reduces Fe-S enzyme activity both in mitochondria and cytosol of mammalian cells. J. Biol. Chem. **281:**25398–25406.
10. **Frishman, D., and M. W. Hentze.** 1996. Conservation of aconitase residues revealed by multiple sequence analysis. Implications for structure/function relationships. Eur. J. Biochem. **239:**197–200.
11. **Galy, B., D. Ferring, and M. W. Hentze.** 2005. Generation of conditional alleles of the murine iron regulatory protein (IRP)-1 and -2 genes. Genesis **43:**181–188.
12. **Galy, B., D. Ferring, B. Minana, O. Bell, H. G. Janser, M. Muckenthaler, K. Schumann, and M. W. Hentze.** 2005. Altered body iron distribution and microcytosis in mice deficient for iron regulatory protein 2 (IRP2). Blood **106:**2580–2589.
13. **Galy, B., S. M. Hölter, T. Klopstock, D. Ferring, L. Becker, S. Kaden, W. Wurst, H.-J. Gröne, and M. W. Hentze.** 2006. Iron homeostasis in the brain: complete iron regulatory protein 2 deficiency without symptomatic neurodegeneration in the mouse. Nat. Genet. **38:**967–969.
14. **Gehring, N., M. W. Hentze, and K. Pantopoulos.** 1999. Menadione-induced oxidative stress leads to inactivation of both RNA-binding and aconitase activities of iron regulatory protein-1. J. Biol. Chem. **274:**6219–6225.
15. **Guo, B., J. D. Phillips, Y. Yu, and E. A. Leibold.** 1995. Iron regulates the intracellular degradation of iron regulatory protein 2 by the proteasome. J. Biol. Chem. **270:**21645–21651.
16. **Henderson, B. R., and L. C. Kühn.** 1995. Differential modulation of the RNA-binding proteins IRP1 and IRP2 in response to iron. IRP2 inactivation requires translation of another protein. J. Biol. Chem. **270:**20509–20515.
17. **Hirling, H., B. R. Henderson, and L. C. Kühn.** 1994. Mutational analysis of the [4Fe-4S]-cluster converting iron regulatory factor from its RNA-binding form to cytoplasmic aconitase. EMBO J. **13:**453–461.
18. **Kaptain, S., W. E. Downey, C. Tang, C. Philpott, D. Haile, D. G. Orloff, J. B. Harford, T. A. Rouault, and R. D. Klausner.** 1991. A regulated RNA binding protein also possesses aconitase activity. Proc. Natl. Acad. Sci. USA **88:**10109–10113.
19. **LaVaute, T., S. Smith, S. Cooperman, K. Iwai, W. Land, E. Meyron-Holtz, S. K. Drake, G. Miller, M. Abu-Asab, M. Tsokos, R. Switzer III, A. Grinberg, P. Love, N. Tresser, and T. A. Rouault.** 2001. Targeted deletion of the gene encoding iron regulatory protein-2 causes misregulation of iron metabolism and neurodegenerative disease in mice. Nat. Genet. **27:**209–214.
20. **Lill, R., and U. Muhlenhoff.** 2005. Iron-sulfur-protein biogenesis in eukaryotes. Trends Biochem. Sci. **30:**133–141.
21. **Lobmayr, L., D. G. Brooks, and R. B. Wilson.** 2005. Increased IRP1 activity in Friedreich ataxia. Gene **354:**157–161.
22. **Meyron-Holtz, E. G., M. C. Ghosh, K. Iwai, T. LaVaute, X. Brazzolotto, U. V. Berger, W. Land, H. Ollivierre-Wilson, A. Grinberg, P. Love, and T. A. Rouault.** 2004. Genetic ablations of iron regulatory proteins 1 and 2 reveal why iron regulatory protein 2 dominates iron homeostasis. EMBO J. **23:**386–395.
23. **Mueller, S., and K. Pantopoulos.** 2002. Activation of iron regulatory protein-1 (IRP1) by oxidative stress. Methods Enzymol. **348:**324–337.
24. **Müllner, E. W., B. Neupert, and L. C. Kühn.** 1989. A specific mRNA binding factor regulates the iron-dependent stability of cytoplasmic transferrin receptor mRNA. Cell **58:**373–382.
25. **Ory, D. S., B. A. Neugeboren, and R. C. Mulligan.** 1996. A stable human-derived packaging cell line for production of high titer retrovirus/vesicular stomatitis virus G pseudotypes. Proc. Natl. Acad. Sci. USA **93:**11400–11406.
26. **Pantopoulos, K.** 2004. Iron metabolism and the IRE/IRP regulatory system: an update. Ann. N. Y. Acad. Sci. **1012:**1–13.
27. **Pantopoulos, K., N. Gray, and M. W. Hentze.** 1995. Differential regulation of two related RNA-binding proteins, iron regulatory protein (IRP) and IRP_B. RNA **1:**155–163.
28. **Pantopoulos, K., and M. W. Hentze.** 1995. Rapid responses to oxidative stress mediated by iron regulatory protein. EMBO J. **14:**2917–2924.
29. **Philpott, C. C., D. Haile, T. A. Rouault, and R. D. Klausner.** 1993. Modification of a free Fe-S cluster cysteine residue in the active iron-responsive element-binding protein prevents RNA binding. J. Biol. Chem. **268:**17655–17658.
30. **Pondarre, C., B. B. Antiochos, D. R. Campagna, S. L. Clarke, E. L. Greer, K. M. Deck, A. McDonald, A. P. Han, A. Medlock, J. L. Kutok, S. A. Anderson, R. S. Eisenstein, and M. D. Fleming.** 2006. The mitochondrial ATP-binding cassette transporter Abcb7 is essential in mice and participates in cytosolic iron-sulfur cluster biogenesis. Hum. Mol. Genet. **15:**953–964.
31. **Rouault, T. A.** 2006. The role of iron regulatory proteins in mammalian iron homeostasis and disease. Nat. Chem. Biol. **2:**406–414.
32. **Roy, A., N. Solodovnikova, T. Nicholson, W. Antholine, and W. E. Walden.** 2003. A novel eukaryotic factor for cytosolic Fe-S cluster assembly. EMBO J. **22:**4826–4835.
33. **Seznec, H., D. Simon, C. Bouton, L. Reutenauer, A. Hertzog, P. Golik, V. Procaccio, M. Patel, J. C. Drapier, M. Koenig, and H. Puccio.** 2005. Friedreich ataxia: the oxidative stress paradox. Hum. Mol. Genet. **14:**463–474.
34. **Smith, S. R., S. Cooperman, T. Lavaute, N. Tresser, M. Ghosh, E. Meyron-Holtz, W. Land, H. Ollivierre, B. Jortner, R. Switzer III, A. Messing, and T. A. Rouault.** 2004. Severity of neurodegeneration correlates with compromise of iron metabolism in mice with iron regulatory protein deficiencies. Ann. N. Y. Acad. Sci. **1012:**65–83.
35. **Smith, S. R., M. C. Ghosh, H. Ollivierre-Wilson, W. Hang Tong, and T. A. Rouault.** 2006. Complete loss of iron regulatory proteins 1 and 2 prevents viability of murine zygotes beyond the blastocyst stage of embryonic development. Blood Cells Mol. Dis. **36:**283–287.
36. **Stehling, O., H. P. Elsasser, B. Bruckel, U. Muhlenhoff, and R. Lill.** 2004. Iron-sulfur protein maturation in human cells: evidence for a function of frataxin. Hum. Mol. Genet. **13:**3007–3015.
37. **Tang, C. K., J. Chin, J. B. Harford, R. D. Klausner, and T. A. Rouault.** 1992. Iron regulates the activity of the iron-responsive element binding protein without changing its rate of synthesis or degradation. J. Biol. Chem. **267:**24466–24470.
38. **Tong, W. H., and T. A. Rouault.** 2006. Functions of mitochondrial ISCU and cytosolic ISCU in mammalian iron-sulfur cluster biogenesis and iron homeostasis. Cell Metab. **3:**199–210.
39. **Wang, J., G. Chen, M. Muckenthaler, B. Galy, M. W. Hentze, and K. Pantopoulos.** 2004. Iron-mediated degradation of IRP2: an unexpected pathway involving a 2-oxoglutarate-dependent oxygenase activity. Mol. Cell. Biol. **24:**954–965.
40. **Wang, J., C. Fillebeen, G. Chen, B. Andriopoulos, and K. Pantopoulos.** 2006. Sodium nitroprusside promotes IRP2 degradation via an increase in intracellular iron and in the absence of S nitrosylation at C178. Mol. Cell. Biol. **26:**1948–1954.
41. **Wang, J., and K. Pantopoulos.** 2002. Conditional derepression of ferritin synthesis in cells expressing a constitutive IRP1 mutant. Mol. Cell. Biol. **22:**4638–4651.
42. **Wingert, R. A., J. L. Galloway, B. Barut, H. Foott, P. Fraenkel, J. L. Axe, G. J. Weber, K. Dooley, A. J. Davidson, B. Schmidt, B. H. Paw, G. C. Shaw, P. Kingsley, J. Palis, H. Schubert, O. Chen, J. Kaplan, and L. I. Zon.** 2005. Deficiency of glutaredoxin 5 reveals Fe-S clusters are required for vertebrate haem synthesis. Nature **436:**1035–1039.
43. **Yikilmaz, E., T. A. Rouault, and P. Schuck.** 2005. Self-association and ligand-induced conformational changes of iron regulatory proteins 1 and 2. Biochemistry **44:**8470–8478.